

PAPER

# Path-integrals and optimal paths for the fractional Ornstein–Uhlenbeck process

To cite this article: Bing Miao *et al* 2026 *J. Phys. A: Math. Theor.* **59** 105004

View the [article online](#) for updates and enhancements.



## You may also like

- [Crossover from anomalous to normal diffusion: truncated power-law noise correlations and applications to dynamics in lipid bilayers](#)  
Daniel Molina-Garcia, Trifce Sandev, Hadiseh Safdari *et al.*
- [Power Brownian Motion: an Ornstein–Uhlenbeck lookout](#)  
Iddo Eliazar
- [Generalised Ornstein–Uhlenbeck process: memory effects and resetting](#)  
P Trajanovski, P Jolakoski, L Kocarev *et al.*



## PAPER

## Path-integrals and optimal paths for the fractional Ornstein–Uhlenbeck process

RECEIVED  
3 December 2025REVISED  
28 January 2026ACCEPTED FOR PUBLICATION  
4 March 2026PUBLISHED  
12 March 2026Bing Miao<sup>1,\*</sup> , Gleb Oshanin<sup>2</sup>  and Luca Peliti<sup>3</sup> <sup>1</sup> University of Chinese Academy of Sciences (UCAS), Beijing 100049, People's Republic of China<sup>2</sup> Sorbonne Université, CNRS, Laboratoire de Physique Théorique de la Matière Condensée (UMR CNRS7600), 4 place Jussieu, 75252 Paris Cedex 05, France<sup>3</sup> Santa Marinella Research Institute, I-00058 Santa Marinella, Italy

\* Author to whom any correspondence should be addressed.

E-mail: [bmiao@ucas.ac.cn](mailto:bmiao@ucas.ac.cn)**Keywords:** path-integral representations, fractional Ornstein–Uhlenbeck process, fractional Gaussian noise, action-minimizing paths**Abstract**

We derive the path-integral representation of the fractional Ornstein–Uhlenbeck process driven by nonstationary Riemann–Liouville fractional Gaussian noise (fGn), for both the subdiffusive and superdiffusive regimes. We express the corresponding action, which is a quadratic functional of individual trajectories of the process, in two alternative but equivalent forms: either in terms of fractional integrals or as a double integral with a nonlocal kernel. Moreover, we determine in closed form the optimal (action-minimizing) paths conditioned to reach a prescribed point at a fixed time moment and discuss their behavior, which appears to be non-intuitive for subdiffusive processes in the presence of a strong confining potential. We also demonstrate that such a behavior persists in case of a stationary fGn in the sense of Mandelbrot and van Ness.

**1. Introduction**

The Ornstein–Uhlenbeck process (OUP) was first introduced to describe velocity fluctuations of a Brownian particle under linear damping [1–3]. It also models the motion of overdamped particles in optical traps [4] or tethered to polymer backbones [5]. As the simplest Gaussian Markov process driven by white noise, the OUP offers a canonical example of mean-reverting relaxation. Its tractability and explicit correlations have made it a standard model in statistical physics and stochastic thermodynamics [6–8], with applications extending to finance, evolutionary dynamics, neuroscience, and climate modeling. Recent work [9, 10] further analyzed its stochastic properties and highlighted a broad scientific relevance of the OUP.

In diverse complex systems such as viscoelastic media, cells, turbulence, finance, and climate, the driving noise often deviates strongly from Gaussian white noise [11, 12]. An extensively studied generalization of the OUP replaces the white-noise term with fractional Gaussian noise (fGn) [13, 14], which exhibits long-range temporal correlations characterized by the Hurst exponent  $H$ . The resulting fractional OUP (fOUP) is non-Markovian and incorporates memory effects relevant to several forms of experimentally observed anomalous diffusion. Depending on  $H$ , the fOUP displays subdiffusive ( $H < 1/2$ ) or superdiffusive ( $H > 1/2$ ) behavior, making it a suitable model for correlated stochastic relaxation in diverse physical, biological, and environmental settings. Consequently, its statistical properties and dynamical features have been the subject of substantial analytical and numerical studies (see, e.g. [15–20]).

The analysis of single-trajectory properties of fGn-driven non-Markovian processes through path-integral representations has recently received substantial attention. Path-integral methods offer a general formalism for stochastic dynamics, linking probabilistic descriptions with techniques from statistical field theory and quantum mechanics [21–27]. They provide alternative approaches to computing correlation

functions and allow for a systematic treatment of memory effects, external perturbations, and dynamical constraints. Within this framework, path-integral formulations have been developed for the trajectories of tagged beads in Gaussian polymer chains [28] — a subdiffusive process with Hurst exponent  $H = 1/4$  — as well as for several variants of *unconstrained* fractional Brownian motion [29–33]. This line of work led to the recent study [34], which used the general form from [33] to derive a path-integral representation of the fOUP driven by stationary fGn in the sense of Mandelbrot and van Ness [13]. This analysis has been also performed for the unusual regime with  $H \in (-1/2, 0)$  [35].

In this paper, we complete the picture deriving a path-integral representation of the fOUP driven by *nonstationary* Riemann–Liouville fGn as defined by Lévy [36]—an alternative and widely used construction of fGn on a finite time  $t$  interval  $t \in (0, T)$ , which is thus more suitable to investigate optimal problems on a finite time interval as compared to the Mandelbrot and van Ness fGn in which  $t$  is defined on the entire real line [13]. We obtain two equivalent formulations of the action: one expressed explicitly in terms of fractional integrals [37], and another written as a double integral with a nonlocal kernel. In addition, building on the general framework developed in [38], we derive explicit closed-form expressions for the optimal (action-minimizing) trajectories of the fOUP conditioned to reach a prescribed point  $X > 0$  at time  $T'$ , and analyze their qualitative behaviors. In particular, we show that in the subdiffusive regime and for sufficiently strong confining potentials, the optimal paths display a counterintuitive behavior: rather than approaching the target monotonically, they initially move away from  $X$ , then reverse direction, and finally reach the target in a rapid terminal excursion. We further demonstrate that such a reversal of motion also occurs for the fOUP driven by *stationary* fGn with time  $t$  defined on the entire real line, i.e. the original Mandelbrot–van Ness fGn [13]. In this case, the reversal of a direction of motion takes place at intermediate times. Overall, the occurrence of such reversals of direction at some stage of the evolution appears to be a generic feature, rooted in the strong antipersistence of the underlying noise.

The paper is structured as follows: In section 2 we formulate our model and introduce basic notations. In section 3 we present the derivation of the action in two alternative forms: in terms of fractional integrals and as a double integral with a non-local kernel. In section 4 we discuss the behavior of the optimal paths. Finally, in section 5 we conclude with a brief recapitulation of our results. For completeness, the derivation of the covariance function of the nonstationary Riemann–Liouville fOUP is provided in appendix A, while appendix B contains the corresponding derivation for the fOUP driven by stationary Mandelbrot–van Ness fGn.

## 2. fOUP with Riemann–Liouville fGn

Consider a stochastic differential equation of the form

$$\gamma \dot{x}_t = -\kappa x_t + \xi_t, \quad x_{t=0} = \dot{x}_{t=0} = 0, \quad (1)$$

where the dot denotes the time derivative and  $\xi_t$  is the Riemann–Liouville fGn (RL fGn), defined by

$$\xi_t = \dot{R}_t^{(H)} = \frac{1}{\Gamma(H+1/2)} \frac{d}{dt} \int_0^t \frac{\zeta_\tau d\tau}{(t-\tau)^{1/2-H}}, \quad (2)$$

where  $H \in (0, 1)$  is the Hurst index,  $R_t^{(H)}$  is a given trajectory of the Riemann–Liouville fractional Brownian motion (RL fBm), first introduced in [36] (see also [39] and references therein), and  $\zeta_\tau$  is a Gaussian white noise with zero mean and the covariance function

$$\overline{\zeta_\tau \zeta_{\tau'}} = 2D\delta(\tau - \tau'). \quad (3)$$

In the latter expression and henceforth the bar denotes averaging over realizations of the Gaussian noise and  $D$  is its intensity. We choose throughout the unit of time such that  $\gamma = 1$ .

The stochastic process defined in equation (1), driven by the non-stationary fGn of equation (2), constitutes the primary focus of our study, for which we aim to derive an exact path-integral representation of its individual trajectories  $x_t$ . We note that the statistical properties of the corresponding process driven by *stationary* fGn, as defined by Mandelbrot and van Ness [13], have been extensively investigated in both mathematical [15, 16] and physical contexts (see, e.g. [9, 17, 18]). The path-integral representation for the fOUP driven by the Mandelbrot and van Ness fGn was recently discussed in [34].

The fOUP  $x_t$  in equation (1) is a zero-mean Gaussian stochastic process and its statistical properties are entirely defined by its covariance function  $\text{cov}_x(t, t')$ . To determine this property, consider first the

covariance function of the RL fBm  $R_t^{(H)}$  defined in equation (2), which obeys, for arbitrary  $t, t'$  and  $H$ ,

$$\begin{aligned} \text{cov}_R(t, t') &= \overline{R_t^{(H)} R_{t'}^{(H)}} \\ &= \frac{2D}{\Gamma^2(H+1/2)} \int_0^m \frac{d\tau}{[(t-\tau)(t'-\tau)]^{1/2-H}}, \quad m = \min(t, t'). \end{aligned} \tag{4}$$

The above integral can be performed for arbitrary  $t, t'$  and  $H$  to give (see, e.g. [29])

$$\begin{aligned} \text{cov}_R(t, t') &= \frac{2Dm^{H+1/2}M^{H-1/2}}{(H+1/2)\Gamma^2(H+1/2)} \\ &\quad \times {}_2F_1\left(1/2-H, 1; H+3/2; \frac{m}{M}\right), \quad M = \max(t, t'), \end{aligned} \tag{5}$$

where  ${}_2F_1$  is Gauss' hypergeometric function. Setting  $t' = t$ , one finds that the mean-square displacement (MSD) of the RL fBm  $R_t^{(H)}$  obeys, for any  $t$ ,

$$\overline{(R_t^{(H)})^2} = \frac{D}{H\Gamma^2(H+1/2)} t^{2H}. \tag{6}$$

For  $H > 1/2$ , the dynamics of the process is superdiffusive, characterized by persistent temporal correlations whereby successive increments tend to maintain the same sign. In this regime, the MSD grows faster than linearly with time. The special case  $H = 1/2$  corresponds to standard Brownian motion, for which correlations vanish and the MSD increases linearly. In contrast, for  $H < 1/2$ , the RL fBm exhibits subdiffusive or antipersistent behavior, characterized by *negatively* correlated increments and a slower-than-linear growth of the MSD.

Note then that the covariance function of the RL fGn in equation (2) formally obeys

$$\text{cov}_\xi(t, t') = \frac{\partial^2}{\partial t \partial t'} \text{cov}_R(t, t'), \tag{7}$$

and is a *bona fide* function only for  $H \geq 1/2$ . For  $H = 1/2$  the covariance is the delta-function, as it should be, while for  $H < 1/2$  the situation is quite delicate: here, the second derivative in equation (7) produces non-integrable diagonal singularities and must be interpreted only distributionally (or as a bilinear form on test functions). However, integrating that distribution against smooth kernels regularizes it and yields finite covariances of positions  $x_t$  of the process in equation (1) (see, e.g. [40]).

Respectively, the covariance function of the process  $x_t$  is given by

$$\text{cov}_x(t, t') = \overline{x_t x_{t'}} = \frac{1}{\gamma^2} e^{-(t+t')/\tau^*} \int_0^t d\tau_1 e^{\tau_1/\tau^*} \int_0^{t'} d\tau_2 e^{\tau_2/\tau^*} \text{cov}_\xi(\tau_1, \tau_2), \tag{8}$$

where  $\tau^*$  is the natural time scale,  $\tau^* = \gamma/\kappa$ , where  $\gamma = 1$  in our units. Using equation (7) and the Beta-integral-type definition in equation (4), expression (8) can be cast into a simpler form (see appendix A),

$$\text{cov}_x(t, t') = \frac{2D}{\Gamma^2(H+1/2)\gamma^2} \int_0^m d\tau \frac{{}_1F_1\left(1, H+1/2, -\frac{t-\tau}{\tau^*}\right) {}_1F_1\left(1, H+1/2, -\frac{t'-\tau}{\tau^*}\right)}{[(t-\tau)(t'-\tau)]^{1/2-H}}, \tag{9}$$

where  ${}_1F_1$  is the confluent hypergeometric function. The expression (9) is formally valid for any  $t, t'$  and  $H$  and is more amenable to analytical and numerical analyses than the one in equation (8). Correspondingly, the MSD is given by

$$\overline{x_t^2} = \frac{2D}{\Gamma^2(H+1/2)\gamma^2} \int_0^t d\tau \frac{{}_1F_1^2\left(1, H+1/2, -\frac{t-\tau}{\tau^*}\right)}{(t-\tau)^{1-2H}}. \tag{10}$$

Alternative representations of the covariance function and the MSD in terms of the Mittag–Leffler function are presented in appendix A.

The integral in equation (10) cannot be performed in an explicit form but its asymptotic behavior in the limit  $t \rightarrow \infty$  can be readily determined to give

$$\overline{x_t^2} = \frac{(\tau^*)^{2H}}{\sin(\pi H)} \frac{D}{\gamma^2} + O\left(e^{-t/\tau^*}\right). \tag{11}$$

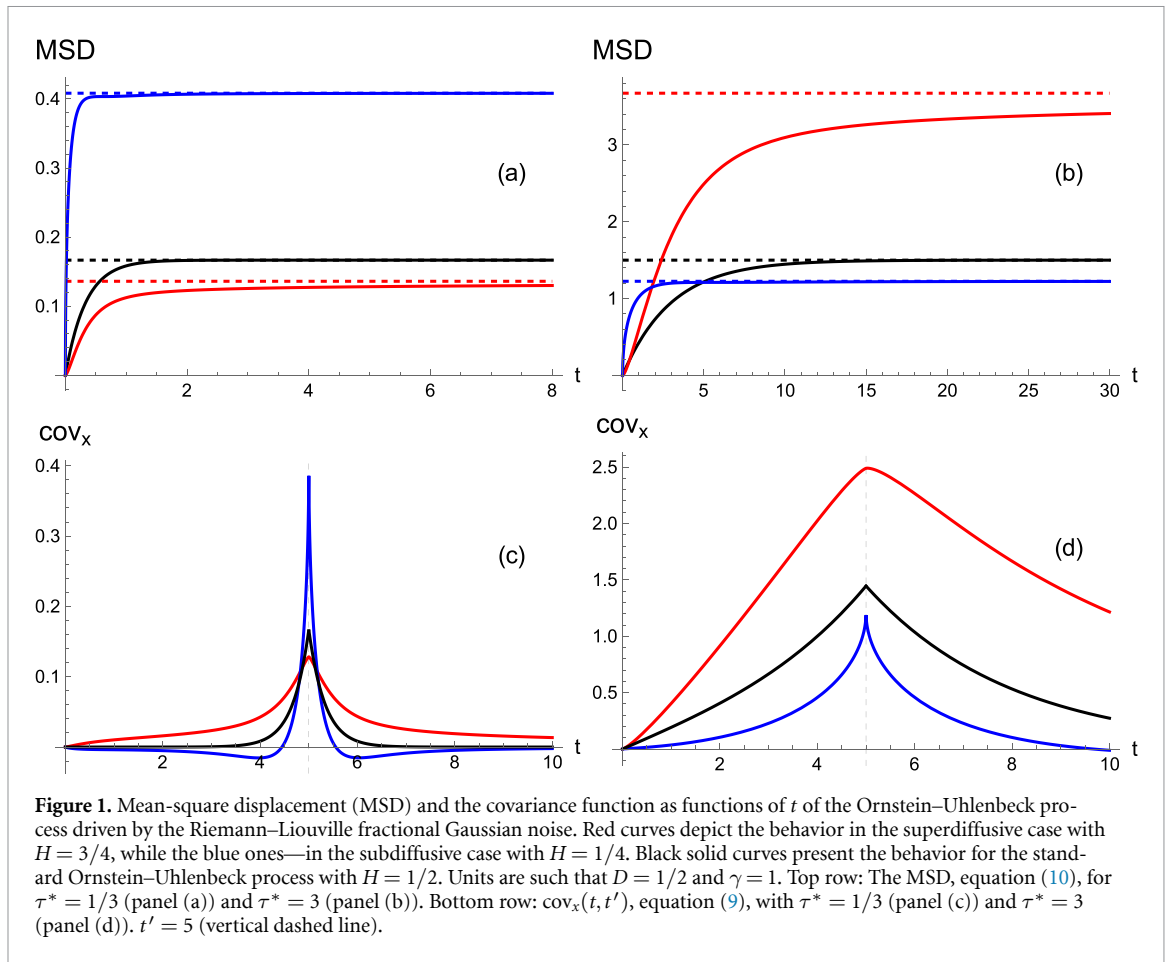


**Figure 1.** Mean-square displacement (MSD) and the covariance function as functions of  $t$  of the Ornstein–Uhlenbeck process driven by the Riemann–Liouville fractional Gaussian noise. Red curves depict the behavior in the superdiffusive case with  $H = 3/4$ , while the blue ones—in the subdiffusive case with  $H = 1/4$ . Black solid curves present the behavior for the standard Ornstein–Uhlenbeck process with  $H = 1/2$ . Units are such that  $D = 1/2$  and  $\gamma = 1$ . Top row: The MSD, equation (10), for  $\tau^* = 1/3$  (panel (a)) and  $\tau^* = 3$  (panel (b)). Bottom row:  $\text{cov}_x(t, t')$ , equation (9), with  $\tau^* = 1/3$  (panel (c)) and  $\tau^* = 3$  (panel (d)).  $t' = 5$  (vertical dashed line).

This expression shows that the MSD relaxes exponentially in time to a finite asymptotic value that depends nontrivially on the time-scale  $\tau^*$ ; namely, for  $\tau^* > 1$ , (i.e.  $\gamma > \kappa$ ), the limiting MSD increases with the Hurst exponent  $H$ , attaining larger values in the superdiffusive regime than in the subdiffusive one. In contrast, for  $\tau^* < 1$ , (i.e.  $\gamma < \kappa$ ), the asymptotic MSD decreases with  $H$ , so that subdiffusive dynamics yield larger stationary fluctuations than superdiffusive ones. The same functional dependence on  $\tau^*$  arises for the fOUP driven by the nonstationary one-sided fGn (defined for  $t \geq 0$ ) introduced by Mandelbrot and van Ness (see, e.g. [17]), as well as for the fOUP driven by a stationary two-sided fGn,  $-\infty < t < \infty$ , (see appendix B).

Figure 1 shows the MSD and the covariance function as functions of time for two values of the characteristic time scale,  $\tau^* = 1/3$  and  $\tau^* = 3$ . For each case, we compare a subdiffusive process with  $H = 1/4$  (blue curves) and a superdiffusive one with  $H = 3/4$  (red curves), along with the classical OUP corresponding to  $H = 1/2$  (black curves). The MSD clearly illustrates the trend described above: when  $\tau^* < 1$ , the MSD is larger in the subdiffusive regime than in the superdiffusive one, whereas for  $\tau^* > 1$  the ordering is reversed. The behavior of the covariance function is more nuanced. For  $\tau^* < 1$ , the same ordering holds only when  $t$  and  $t'$  are close to one another (the region that determines the MSD), while for sufficiently different  $t$  and  $t'$  the covariance in the subdiffusive case becomes smaller than in the superdiffusive case. For  $\tau^* > 1$ , by contrast, the covariance function corresponding to the superdiffusive process remains larger for all times  $t$  and  $t'$ . A notable feature in the subdiffusive case, particularly visible in figure 1(a), is the appearance of negative lobes in the covariance function away from the diagonal  $t = t'$ . This sign change is not an artefact but a direct manifestation of anti-persistence in the driving fGn: correlations at different times tend to oppose each other, and the fOUP inherits this behavior. Similar negative covariance regions are also known for fOUP driven by the stationary fGn of Mandelbrot and van Ness (see, e.g. [34]). We will show below that the presence of such negative lobes induces quite a non-trivial behavior of the action-minimizing paths.

### 3. Path-integral representations of the fOUP

Using the definition in equation (2) we rewrite formally equation (1) as

$$\frac{1}{\Gamma(H+1/2)} \int_0^t \frac{\zeta_\tau d\tau}{(t-\tau)^{1/2-H}} = K_t, \quad K_t = \int_0^t d\tau (\gamma \dot{x}_\tau + \kappa x_\tau). \tag{12}$$

This is Abel’s integral equation which can be solved exactly by applying to both sides of this equation (from the left) an appropriate inverse Riemann–Liouville operator (see [37, p 29]), which gives

$$\zeta_t = \frac{1}{\Gamma(1/2-H)} \frac{d}{dt} \int_0^t \frac{K_\tau d\tau}{(t-\tau)^{H+1/2}} = \left(\mathcal{D}_+^{H+1/2} K\right)(t), \tag{13}$$

where the operator  $\mathcal{D}_+^{H+1/2} K$  in the right-hand-side (rhs) of equation (13) denotes the so-called *fractional* Riemann–Liouville derivative of order  $H+1/2$  acting on the function  $K$  (see the definition 2.2 in [37, p. 35]). The subscript ‘+’ signifies that a left-sided fractional derivative is used, meaning that the time variable appears as the upper limit of integration in the corresponding fractional operator.

For subdiffusive (antipersistent) noise the order  $H+1/2$  of the fractional derivative is less than 1. In this case, we have (see [37, p 25, equation (2.24)])

$$\left(\mathcal{D}_+^{H+1/2} K\right)(t) = \frac{1}{\Gamma(1/2-H)} \left[ \frac{K_0}{t^{H+1/2}} + \int_0^t \frac{\dot{K}_\tau d\tau}{(t-\tau)^{H+1/2}} \right], \tag{14}$$

where the first term in the brackets evidently vanishes because  $K_{t=0} \equiv 0$ . Consequently, for subdiffusive fractional RL fGn one has

$$\zeta_t = \left(\mathcal{D}_+^{H+1/2} K\right)(t) = \frac{1}{\Gamma(1/2-H)} \int_0^t \frac{(\gamma \dot{x}_\tau + \kappa x_\tau) d\tau}{(t-\tau)^{H+1/2}}. \tag{15}$$

For superdiffusive (persistent) noise the order  $H+1/2$  of the fractional derivative is greater than 1 and can be written as  $H+1/2 = 1 + (H-1/2)$ . We take advantage of the representation in [37, equation (2.43)] to get

$$\begin{aligned} \left(\mathcal{D}_+^{H+1/2} K\right)(t) &= \frac{K_0}{\Gamma(1/2-H) t^{H+1/2}} + \frac{\dot{K}_0}{\Gamma(3/2-H) t^{H-1/2}} \\ &+ \frac{1}{\Gamma(3/2-H)} \int_0^t \frac{\ddot{K}_\tau d\tau}{(t-\tau)^{H-1/2}}. \end{aligned} \tag{16}$$

The first term in the rhs of the latter expression is identically equal to zero, while the second one vanishes because of the initial conditions we have chosen. Consequently, for the superdiffusive RL fGn we get

$$\zeta_t = \left(\mathcal{D}_+^{H+1/2} K\right)(t) = \frac{1}{\Gamma(3/2-H)} \int_0^t \frac{(\gamma \ddot{x}_\tau + \kappa \dot{x}_\tau) d\tau}{(t-\tau)^{H-1/2}}. \tag{17}$$

Lastly, the probability functional for observing a given realization of Gaussian white noise  $\zeta_t$  on a finite time interval  $(0, T)$  is

$$P[\zeta_t] \simeq \exp\left(-\frac{1}{4D} \int_0^T dt \zeta_t^2\right), \tag{18}$$

where the symbol  $\simeq$  here and henceforth signifies equality up to a multiplicative normalization constant, which does not influence the functional form of the action nor the resulting optimal paths. The above expression is central for our further analysis of the form of the probability  $P[x_t]$  of observing a given trajectory  $x_t$  of the fOUP on the interval  $(0, T)$ . Taking advantage of equation (18) and equations (15) and (17), we derive below the desired path-integrals representations of fOUP.

### 3.1. Path-integral representations in terms of fractional integrals

We seek first an exact representation of  $P[x_t]$  with an action written in terms of fractional integrals, which can be done very straightforwardly by merely using equation (13). We find then that the probability of observing on the time-interval  $(0, T)$  a given realization  $x_t$  of the process obeying equation (1) is formally given by

$$P[x_t] \simeq \exp\left(-\frac{1}{4D} \int_0^T dt \left[ \left( \mathcal{D}_+^{H+1/2} K \right) (t) \right]^2\right). \tag{19}$$

Further on, taking advantage of expressions (15) and (17), we find

$$P[x_t] \simeq \exp\left(-\frac{1}{4D} \int_0^T dt \left[ \frac{1}{\Gamma(1/2-H)} \int_0^t \frac{(\gamma \dot{x}_\tau + \kappa x_\tau) d\tau}{(t-\tau)^{H+1/2}} \right]^2\right), \tag{20}$$

$$P[x_t] \simeq \exp\left(-\frac{1}{4D} \int_0^T dt \left[ \frac{1}{\Gamma(3/2-H)} \int_0^t \frac{(\gamma \ddot{x}_\tau + \kappa \dot{x}_\tau) d\tau}{(t-\tau)^{H-1/2}} \right]^2\right),$$

for the subdiffusive and superdiffusive cases, respectively.

Three remarks regarding the expressions in equations (20) are in order:

First, setting  $\kappa = 0$  one recovers known results for unconstrained dynamics. In this limit, the first line of equation (20) reduces to the classical action for the RL fBm obtained in [29], while the second line coincides with the superdiffusive result reported in [32].

Second, the appearance of second-order derivatives in the action for the superdiffusive regime is expected: such terms arise naturally in systems with bending rigidity, such as semiflexible polymers and membranes [26], for random acceleration process [27], and for unconstrained superdiffusive fractional Brownian motions [32, 33]. Importantly, although individual fractional Brownian trajectories are almost surely nowhere differentiable, the appearance of first- or second-order time derivatives in the action does not imply any assumption of pathwise smoothness. Rather, these derivatives originate from the structure of the inverse covariance operator and must be understood in a weak, quadratic-form sense within the Gaussian path measure. The action thus specifies how fluctuations are weighted statistically, not how typical paths behave pointwise. The change in the order of derivatives between the subdiffusive and superdiffusive regimes reflects the different scaling of temporal correlations encoded in the covariance, ensuring that the path-integral formulation remains both mathematically consistent and physically meaningful.

Third, we consider the limit  $H \rightarrow 1/2$ , i.e. the case of a white noise. In the superdiffusive case (second line in equation (20)) we can straightforwardly set  $H = 1/2$  in the fractional integral to get

$$P[x_t] \simeq \exp\left(-\frac{1}{4D} \int_0^T dt \left[ \int_0^t (\gamma \ddot{x}_\tau + \kappa \dot{x}_\tau) d\tau \right]^2\right) \tag{21}$$

$$\simeq \exp\left(-\frac{1}{4D} \int_0^T dt (\gamma \dot{x}_t + \kappa x_t)^2\right),$$

which is the exact result for the standard OUP driven by a Gaussian white noise. In the subdiffusive case the passage  $H \rightarrow 1/2$  is a bit more delicate and cannot be performed directly in the integral. To this end, we first formally rewrite the fractional integral as

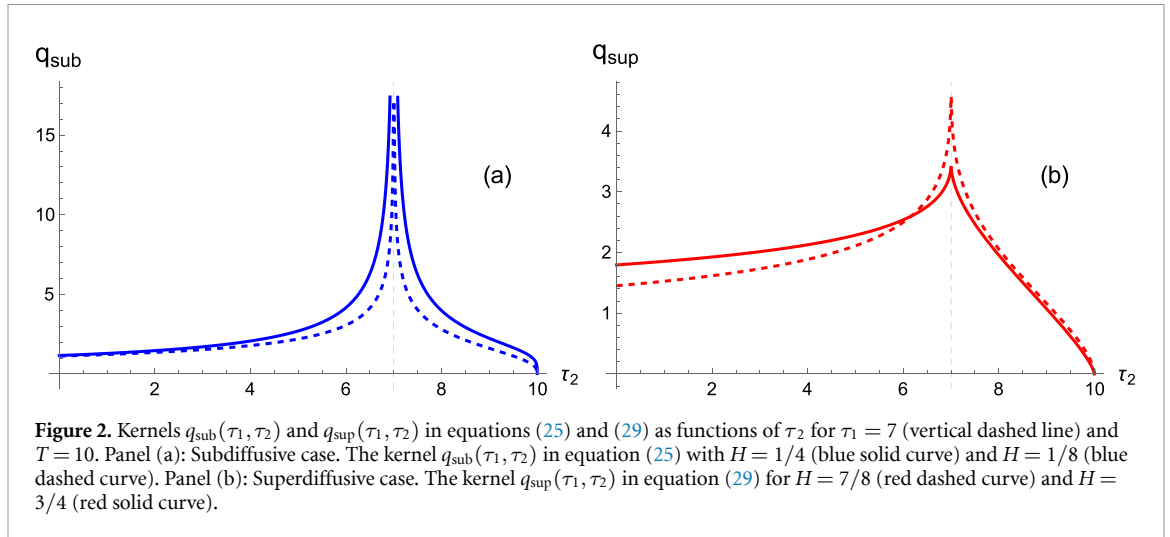
$$\frac{1}{\Gamma(1/2-H)} \int_0^t \frac{(\gamma \dot{x}_\tau + \kappa x_\tau) d\tau}{(t-\tau)^{H+1/2}} = -\frac{1}{\Gamma(3/2-H)} \int_0^t (\gamma \dot{x}_\tau + \kappa x_\tau) d\tau \frac{d}{d\tau} (t-\tau)^{1/2-H}, \tag{22}$$

and then perform the integral in the right-hand-side by parts assuming that  $H < 1/2$ , i.e.  $H$  is bounded away from  $1/2$ . This gives

$$-\frac{1}{\Gamma(3/2-H)} \int_0^t (\gamma \dot{x}_\tau + \kappa x_\tau) d\tau \frac{d}{d\tau} (t-\tau)^{1/2-H} \tag{23}$$

$$= \frac{1}{\Gamma(3/2-H)} \int_0^t (\gamma \ddot{x}_\tau + \kappa \dot{x}_\tau) (t-\tau)^{1/2-H} d\tau,$$

in which we can now safely put  $H = 1/2$  to get the expression (21).



### 3.2. Path-integral representations with non-local kernels

We now focus on the path-integral representation in which the action takes a more standard form of the double integral with a non-local kernel. Changing the integration order in equation (20) and performing the inner integral over  $t$ , we have that in case of a subdiffusive fOUP  $P[x_i]$  attains the form

$$P[x_i] \simeq \exp \left( -\frac{1}{4D\Gamma^2(1/2-H)} \int_0^T d\tau_1 (\gamma \dot{x}_{\tau_1} + \kappa x_{\tau_1}) \times \int_0^T d\tau_2 (\gamma \dot{x}_{\tau_2} + \kappa x_{\tau_2}) q_{\text{sub}}(\tau_1, \tau_2) \right), \tag{24}$$

where the kernel  $q_{\text{sub}}(\tau_1, \tau_2)$  is a function of  $\tau_1$  and  $\tau_2$  which is given explicitly by

$$q_{\text{sub}}(\tau_1, \tau_2) = \frac{1}{|\tau_1 - \tau_2|^{2H}} B_z(1/2 - H, 2H), \quad z = \frac{T - \max(\tau_1, \tau_2)}{T - \min(\tau_1, \tau_2)}, \tag{25}$$

where  $B_z(a, b)$  is the incomplete Beta function:

$$B_z(a, b) = \int_0^z dx x^{a-1} (1-x)^{b-1}. \tag{26}$$

We depict  $q_{\text{sub}}$  as function of  $\tau_2$  (with fixed  $\tau_1$ ) in the left panel in figure 2. We observe that  $q_{\text{sub}}$  tends to a computable constant when  $\tau_2 \rightarrow 0$ , vanishes when  $\tau_2 \rightarrow T$  and diverges when  $\tau_2 \rightarrow \tau_1$ ,

$$q_{\text{sub}}(\tau_1, \tau_2) \simeq \frac{\Gamma(1/2-H)\Gamma(2H)}{\Gamma(1/2+H)} \frac{1}{|\tau_1 - \tau_2|^{2H}}. \tag{27}$$

The divergence is stronger the closer  $H$  is to  $1/2$ .

Consider next the case of superdiffusion. Performing essentially the same procedure, we get

$$P[x_i] \simeq \exp \left( -\frac{1}{4D\Gamma^2(3/2-H)} \int_0^T d\tau_1 (\gamma \ddot{x}_{\tau_1} + \kappa \dot{x}_{\tau_1}) \times \int_0^T d\tau_2 (\gamma \ddot{x}_{\tau_2} + \kappa \dot{x}_{\tau_2}) q_{\text{sup}}(\tau_1, \tau_2) \right), \tag{28}$$

where the kernel  $q_{\text{sup}}(\tau_1, \tau_2)$  obeys

$$q_{\text{sup}}(\tau_1, \tau_2) = |\tau_1 - \tau_2|^{2-2H} B_z(3/2 - H, 2H - 2). \tag{29}$$

This kernel is depicted as function of  $\tau_2$  (for fixed  $\tau_1$ ) in figure 2. Likewise in the subdiffusive case,  $q_{\text{sup}}$  tends to a computable constant when  $\tau_2 \rightarrow 0$  and vanishes when  $\tau_2 \rightarrow T$ . In contrast to the subdiffusive case,  $q_{\text{sup}}$  approaches a constant value when  $\tau_2 \rightarrow \tau_1$ . Indeed, the Beta function in equation (29) diverges as

$$B_z(3/2 - H, 2H - 2) \simeq \frac{(3 - 2H)}{4(1 - H)} (1 - z)^{2H-2}, \quad z \rightarrow 1, \tag{30}$$

and consequently,

$$\lim_{\tau_2 \rightarrow \tau_1} q_{\text{sup}}(\tau_1, \tau_2) = \frac{(3 - 2H)}{4(1 - H)} (T - \tau_1)^{2(1-H)}. \tag{31}$$

Therefore, for  $\tau_2 = \tau_1$  and finite  $T$  the kernel has a finite-height peak when the arguments coincide. The height of the peak depends on  $\tau_1$  and  $T$ .

### 4. Optimal paths

Consider such paths  $x_t^*$  which start at 0 at  $t = 0$ , appear at position  $X$  at time instant  $T' < T$ , and provide the minimum value to the actions in equations (24) or (28); that being,  $x_t^*$  are the action-minimizing or ‘optimal’ paths. Our aim is to define  $x_t^*$  explicitly; to this end, we resort to the analysis in recent [38] in which this problem has been solved for arbitrary Gaussian processes which are entirely defined by their covariance function. For completeness, we repeat here the main arguments presented in [38].

Suppose that we rewrite formally, by integration by parts, the actions in equations (24) and (28) in the canonical form

$$S = \frac{1}{4D} \int_0^T d\tau_1 \int_0^T d\tau_2 x_{\tau_1} x_{\tau_2} Q(\tau_1, \tau_2), \tag{32}$$

where  $Q(\tau_1, \tau_2) = Q(\tau_2, \tau_1)$  can be readily expressed in terms of  $q_{\text{sub}}(\tau_1, \tau_2)$  in case of subdiffusion or  $q_{\text{sup}}(\tau_1, \tau_2)$  for the superdiffusive motion. The resulting expressions are quite lengthy and we do not present them here. As a matter of fact, one does not need to know the precise form of this kernel. On the other hand, the kernel  $Q(\tau_1, \tau_2)$  obeys the integral equation [41]

$$\int_0^T d\tau_2 Q(\tau_1, \tau_2) \text{cov}_x(\tau_1', \tau_2) = \delta(\tau_1 - \tau_1'), \tag{33}$$

where  $\text{cov}_x(\tau_1', \tau_2)$  is the covariance function of the process  $x_t$  defined in equation (9). Next, we consider an auxiliary action of the form

$$\tilde{S} = \frac{1}{4D} \int_0^T d\tau_1 \left[ \int_0^T d\tau_2 x_{\tau_1} x_{\tau_2} Q(\tau_1, \tau_2) - \lambda x_{\tau_1} \delta(\tau_1 - T') \right], \tag{34}$$

where the second term in the brackets implements the condition

$$\int_0^T d\tau_1 x_{\tau_1} \delta(\tau_1 - T') = X, \tag{35}$$

while the Lagrange multiplier  $\lambda$  is to be chosen to ensure that  $x_{t=T'} = X$ . Then, the linear variation of the auxiliary action is given by

$$\delta\tilde{S} = \frac{1}{2D} \int_0^T d\tau_1 \delta x_{\tau_1} \left[ \int_0^T d\tau_2 x_{\tau_2} Q(\tau_1, \tau_2) - \frac{\lambda}{2} \delta(\tau_1 - T') \right], \tag{36}$$

and must vanish for arbitrary  $\delta x_{\tau_1}$  which yields a linear integral equation for the optimal paths:

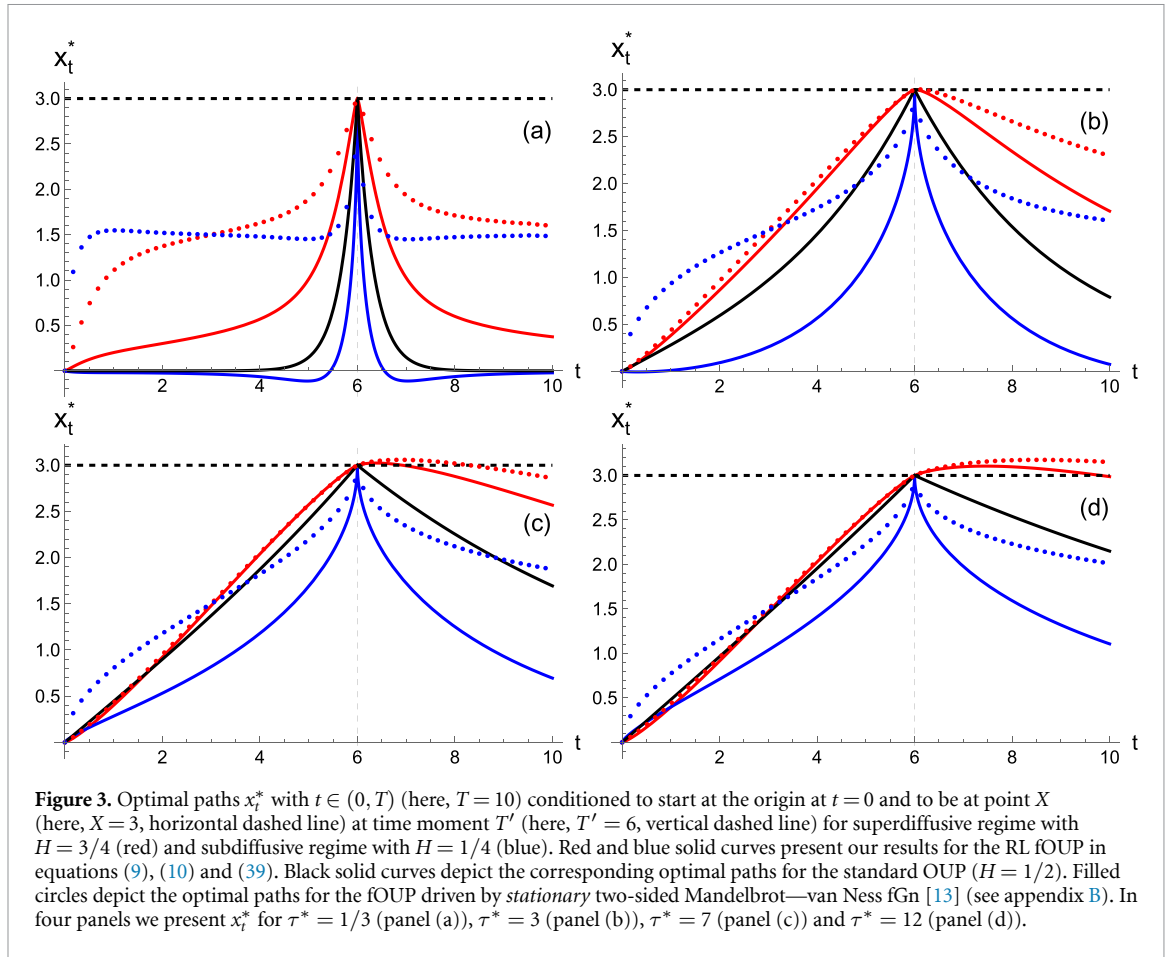
$$\int_0^T d\tau_2 x_{\tau_2}^* Q(\tau_1, \tau_2) = \frac{\lambda}{2} \delta(\tau_1 - T'). \tag{37}$$

Comparing equations (37) and (33) one readily infers that [38]

$$x_t^* = \frac{\lambda}{2} \text{cov}_x(t, T'), \tag{38}$$

and hence, choosing  $\lambda = 2X/\text{cov}_x(T', T')$ , one has that the optimal path from the origin to point  $X$  reached at time instant  $t = T' < T$  obeys

$$x_t^* = \frac{\text{cov}_x(t, T')}{\text{cov}_x(T', T')} X. \tag{39}$$



Note that the above procedure can be readily generalized for the optimal paths constrained to visit point  $X_1$  at time moment  $T_1$ , point  $X_2$  at time moment  $T_2$ , and so on (see [38]).

Figure 3 shows the optimal paths  $x_t^*$  from equations (9), (10) and (39), conditioned to start at the origin at  $t = 0$  and to reach a prescribed point  $X > 0$  at time  $t = T'$ . The red solid curves correspond to the superdiffusive regime ( $H = 3/4$ ), the blue solid curves to the subdiffusive regime ( $H = 1/4$ ), and the black solid curves represent the classical OUP case ( $H = 1/2$ ). The comparison highlights how persistence or anti-persistence of the driving noise affects the structure of the optimal trajectories and makes it different from the OUP case. The four panels of figure 3 correspond to different values of the parameter  $\tau^* = \gamma/\kappa$ :  $\tau^* = 1/3$  (a),  $\tau^* = 3$  (b),  $\tau^* = 7$  (c) and  $\tau^* = 12$  (d). Panels (a) and (b) both correspond to  $\tau^* < T' < T$ , but differ in whether  $\tau^*$  is smaller or larger than unity, leading to qualitatively distinct behaviors. In panel (c), the scales satisfy  $T' < \tau^* < T$ , while in panel (d) one has  $T' < T < \tau^*$ . Since  $\tau^*$  is inversely proportional to the strength of the confining quadratic potential, panel (a) corresponds to the strongest confinement and panel (d) to the weakest.

We begin with the superdiffusive case. In all four panels, the optimal trajectories approach the target monotonically, steadily decreasing their distance to  $X$ . Under strong confinement (panel (a)), the velocity  $\dot{x}_t^*$  varies noticeably in time, while this variation becomes progressively weaker as  $\tau^*$  increases, corresponding to a reduction of the confining strength. One also observes that the optimal fOUP trajectory initially moves more slowly than the classical OUP, but then accelerates at later times (see panels (c) and (d)). After reaching the target, the behavior depends on the confinement strength: in panels (a) and (b), the optimal path subsequently turns back for  $t \geq T'$  toward the origin, whereas in panels (c) and (d) it overshoots, moving further away for a while before eventually reversing direction.

The subdiffusive case under strong confinement displays a markedly nontrivial behavior. Owing to the anti-persistence of the driving noise, the optimal trajectory initially moves *away* from the target, increasing its distance from  $X$ , before abruptly reversing direction, accelerating, and reaching  $X$  within a short time interval. For  $t \geq T'$ , the trajectory departs from the target rapidly, crosses the origin, and then relaxes toward it from below. As the confining potential is weakened (i.e. as  $\tau^*$  increases), this pronounced manifestation of noise anti-correlations gradually disappears: the optimal paths then approach  $X$  monotonically and subsequently drift back toward the origin.

Finally, we examine the impact of the nonstationarity of the driving fGn on the structure of the optimal paths. To this end, in appendix B we consider the fOUP driven by a stationary fGn in the sense of Mandelbrot and van Ness [13], with  $t$  defined on the entire real line. In this formulation, the process is assumed to have evolved since  $t = -\infty$ , to be at the origin at  $t = 0$ , and to subsequently undergo free evolution. Note that although the underlying fGn is stationary in this case, the resulting fOUP becomes nonstationary due to the condition imposed at  $t = 0$ . The corresponding covariance function is derived in appendix B (see also [15, 34] for similar results in somewhat different settings), and the expression (39) remains valid for determining the optimal paths, which start at the origin at  $t = 0$  and are conditioned to reach the position  $X$  at time  $T'$ . These paths are shown in figure 3 by filled blue circles for subdiffusion, as exemplified here by  $H = 1/4$ , and by filled red circles for superdiffusion with  $H = 3/4$ .

We observe that for the strongest confining potential (panel (a) in figure 3) the optimal paths corresponding to stationary and nonstationary noises exhibit distinct behaviors in both the superdiffusive and subdiffusive regimes. In the superdiffusive case, the differences are primarily quantitative: for stationary noise the optimal path moves toward the target more rapidly at early times than in the nonstationary case, subsequently slows down, and finally reaches the target via a rapid terminal excursion. In contrast, in the subdiffusive regime the differences are also qualitative. While in the nonstationary case the optimal path initially moves away from the target, in the stationary case it first goes toward the target, then reverses direction and drifts away from it. As the time instant  $T'$  is approached at which the path has to be at  $X$ , the path undergoes a second reversal and reaches the target in a rapid final excursion. Aside from this detail, the occurrence of a reversal in the direction of motion appears to be a generic feature of the behavior of the optimal path that originates from the strong antipersistence of the underlying noise. As a matter of fact, a change of the direction of motion of the optimal path is also apparent for the Mandelbrot and van Ness fGn in slightly different settings [34] (see the left panel in figure 2 therein). Beyond  $T'$ , the optimal paths for stationary and nonstationary noises also differ markedly in both the subdiffusive and superdiffusive regimes.

Upon weakening the confining potential (panels (b)–(d)), the optimal paths in the superdiffusive regime for stationary and nonstationary noise progressively converge and become almost indistinguishable for sufficiently large  $\tau^*$ . Differences persist for times beyond  $T'$ , but become less pronounced as  $\tau^*$  increases. By contrast, in the subdiffusive regime the optimal paths corresponding to stationary and nonstationary noises remain quantitatively distinct for all values of  $\tau^*$ .

## 5. Conclusions

In conclusion, we have developed a path-integral formulation for the non-Markovian fOUP driven by nonstationary Riemann–Liouville fGn, covering both subdiffusive and superdiffusive regimes. Two equivalent representations of the associated action were obtained. The first expresses the action explicitly in terms of Riemann–Liouville fractional integrals, thereby making the role of fractional operators in the dynamics transparent. The second recasts the action in a more conventional double-integral form, at the expense of introducing a nonlocal kernel that encapsulates the memory inherent in the driving noise.

Within this framework, we further derived closed-form expressions for the optimal (action-minimizing) trajectories of the process conditioned to reach a prescribed position  $X > 0$  at some fixed time instant. The resulting paths were analyzed in detail across several parameter regimes, in particular, for different strengths of the confining potential. Interestingly enough, we found that in the subdiffusive case, and for sufficiently strong confining potentials, the optimal conditioned trajectories exhibit a non-monotonic structure: instead of moving directly toward the target, they initially deviate in the opposite direction before reversing and approaching  $X$  through a rapid final excursion. We have shown that this reversal of the direction of motion in the subdiffusive regime, which originates from the antipersistence of the underlying noise, is also present when the system is driven by stationary Mandelbrot–van Ness fGn. This indicates that a transient ‘overshoot’ away from the target is a robust hallmark of memory-driven relaxation dynamics, and highlights a qualitative distinction between fractional and Markovian OUPs.

Our results provide a systematic foundation for the analysis of conditioned paths in fractional stochastic processes and may prove useful in applications where non-Markovian noise and constrained dynamics play a central role, including viscoelastic transport, intracellular biophysics, and anomalous relaxation in complex media.

### Acknowledgments

The authors wish to thank Baruch Meerson for helpful discussions. BM acknowledges support from the National Natural Science Foundation of China (NSFC) (Grant Nos. 12575045 and 12034019).

### Data availability statement

No new data were created or analysed in this study.

### Appendix A. Covariance function of the nonstationary Riemann–Liouville fractional Ornstein–Uhlenbeck process (fOUP).

We first formally rewrite the definition (4) as

$$\text{cov}_R(\tau_1, \tau_2) = \frac{2D}{\Gamma^2(H+1/2)} \int_0^\infty \frac{d\tau \theta(\tau_1 - \tau) \theta(\tau_2 - \tau)}{[(\tau_1 - \tau)(\tau_2 - \tau)]^{1/2-H}}, \tag{A.1}$$

where  $\theta(t)$  is the Heaviside theta function, which satisfies  $\theta(t) = 1$  for  $t \geq 0$ , and zero otherwise. Inserting the above expression into equation (8) and changing the integration order, we have

$$\begin{aligned} \text{cov}_x(t, t') &= \frac{2D}{\Gamma^2(H+1/2)\gamma^2} e^{-(t+t')/\tau^*} \int_0^\infty d\tau \left\{ \int_0^t d\tau_1 e^{\tau_1/\tau^*} \frac{d}{d\tau_1} \frac{\theta(\tau_1 - \tau)}{(\tau_1 - \tau)^{1/2-H}} \right\} \\ &\times \left\{ \int_0^{t'} d\tau_2 e^{\tau_2/\tau^*} \frac{d}{d\tau_2} \frac{\theta(\tau_2 - \tau)}{(\tau_2 - \tau)^{1/2-H}} \right\}. \end{aligned} \tag{A.2}$$

Next, integrating by parts the terms in the curly brackets, we have

$$\begin{aligned} \int_0^t d\tau_1 e^{\tau_1/\tau^*} \frac{d}{d\tau_1} \frac{\theta(\tau_1 - \tau)}{(\tau_1 - \tau)^{1/2-H}} &= \frac{\theta(t - \tau)}{(t - \tau)^{1/2-H}} e^{t/\tau^*} \\ &\times \left( 1 - \frac{(t - \tau)}{(H + 1/2)\tau^*} {}_1F_1\left(1, H + 3/2, -\frac{(t - \tau)}{\tau^*}\right) \right), \\ \int_0^{t'} d\tau_2 e^{\tau_2/\tau^*} \frac{d}{d\tau_2} \frac{\theta(\tau_2 - \tau)}{(\tau_2 - \tau)^{1/2-H}} &= \frac{\theta(t' - \tau)}{(t' - \tau)^{1/2-H}} e^{t'/\tau^*} \\ &\times \left( 1 - \frac{(t' - \tau)}{(H + 1/2)\tau^*} {}_1F_1\left(1, H + 3/2, -\frac{(t' - \tau)}{\tau^*}\right) \right). \end{aligned} \tag{A.3}$$

Using the identity

$$\frac{z}{b} {}_1F_1(a + 1, b + 1, z) = {}_1F_1(a + 1, b, z) - {}_1F_1(a, b, z), \tag{A.4}$$

and rewriting formally the expressions in the right-hand-side of equation (A.3), we recover our results in equations (9) and (10).

Finally, we note that

$${}_1F_1(1, H + 1/2, z) = \Gamma(H + 1/2) \sum_{n=0}^\infty \frac{z^n}{\Gamma(n + H + 1/2)} = \Gamma(H + 1/2) E_{1, H+1/2}(z), \tag{A.5}$$

where  $E_{1, H+1/2}(z)$  is the Mittag–Leffler function. Correspondingly, the representations of the covariance function and the MSD in equations (9) and (10) can be formally rewritten in terms of  $E_{1, H+1/2}(z)$  as

$$\text{cov}_x(t, t') = \frac{2D}{\gamma^2} \int_0^m d\tau \frac{E_{1, H+1/2}\left(-\frac{t-\tau}{\tau^*}\right) E_{1, H+1/2}\left(-\frac{t'-\tau}{\tau^*}\right)}{[(t - \tau)(t' - \tau)]^{1/2-H}}, \quad m = \min(t, t'), \tag{A.6}$$

and

$$\overline{x_t^2} = \frac{2D}{\gamma^2} \int_0^t d\tau \frac{E_{1, H+1/2}^2\left(-\frac{t-\tau}{\tau^*}\right)}{(t - \tau)^{1-2H}} = \frac{2D}{\gamma^2} (\tau^*)^{2H} \int_0^{t/\tau^*} dz z^{2H-1} E_{1, H+1/2}^2(-z). \tag{A.7}$$

### Appendix B. Covariance function of the two-sided Mandelbrot—van Ness fOUP.

Consider now the case when the time variable  $t$  is defined on the entire real axis (the so-called two-sided case),  $-\infty < t < \infty$ , and replace the noise term  $\xi_t$  in equation (1) by the stationary fGn  $\xi_t^{(MvH)}$  introduced by Mandelbrot and van Ness [13]. Here, the noise  $\xi_t^{(MvH)}$  is defined as the time derivative of a trajectory of the Mandelbrot-van Ness fractional Brownian motion  $R_t^{(MvH)}$ , which is the Gaussian process with zero mean and the covariance function

$$\text{cov}_R^{(MvH)}(t, t') = \overline{R_t^{(MvH)} R_{t'}^{(MvH)}} = D' (|t|^{2H} + |t'|^{2H} - |t - t'|^{2H}), \tag{B.1}$$

where  $D'$  is the proportionality factor with physical dimension  $\text{length}^2/\text{time}^{2H}$  and  $H \in (0, 1)$  is the Hurst index. As above, the covariance function of  $\xi_t^{(MvH)}$  is related to the covariance function  $\text{cov}_R^{(MvH)}(t, t')$  in equation (B.1) via equation (7), and depends only on the absolute value of the time difference  $|t - t'|$ , because the fGn  $\xi_t^{(MvH)}$  is a stationary process. Lastly, we note that the overline in equation (B.1) denotes averaging over realizations of the process  $R_t^{(MvH)}$ —a notation we previously used for averaging over realizations of white noise. Such a notation is appropriate here because  $R_t^{(MvH)}$  is, in fact, a functional of white noise, defined via a Weyl-type stochastic integral [13].

For the case under study the solution of equation (1) with the initial condition  $x_0 = 0$  reads

$$x_t = \frac{1}{\gamma} \int_{-\infty}^t e^{-(t-\tau)/\tau^*} \xi_\tau^{(MvH)} d\tau - \frac{1}{\gamma} \int_{-\infty}^0 e^{\tau/\tau^*} \xi_\tau^{(MvH)} d\tau. \tag{B.2}$$

To compute the covariance function of  $x_t$  in equation (B.2), it is advantageous to use the integral representation of the covariance function in equation (B.1), whereby the kernel attains a factorized dependence on  $t$  and  $t'$ . Specifically, we rewrite each term in equation (B.1) using the integral identity

$$|t|^{2H} = \frac{\sin(\pi H) \Gamma(2H + 1)}{\pi} \int_{-\infty}^{\infty} \frac{|\lambda|^{1-2H}}{\lambda^2} (1 - e^{i\lambda t}) d\lambda, \tag{B.3}$$

which is valid for any  $H \in (0, 1)$ , to get [42]

$$\text{cov}_R^{(MvH)}(t, t') = \frac{\sin(\pi H) \Gamma(2H + 1) D'}{\pi} \int_{-\infty}^{\infty} \frac{|\lambda|^{1-2H}}{\lambda^2} (1 - e^{i\lambda t}) (1 - e^{-i\lambda t'}) d\lambda. \tag{B.4}$$

Then, writing down the formal definition of the covariance of the process  $x_t$  using the relation in equation (7) and the expression (B.4), we get

$$\text{cov}_x^{(MvH)}(t, t') = \frac{\sin(\pi H) \Gamma(2H + 1) D'}{\pi \gamma^2} \int_{-\infty}^{\infty} \frac{|\lambda|^{1-2H}}{(\tau^*)^{-2} + \lambda^2} (1 - e^{i\lambda t}) (1 - e^{-i\lambda t'}) d\lambda. \tag{B.5}$$

Note that in the limit  $\tau^* \rightarrow \infty$ , the above expression reduces to equation (B.4), as it should. Lastly, performing the integral in equation (B.5), we find the following explicit expression for the covariance function of the fOUP  $x_t$ :

$$\text{cov}_x^{(MvH)}(t, t') = \frac{\Gamma(2H + 1) D' (\tau^*)^{2H}}{\gamma^2} (M_H(t) + M_H(t') - M_H(t - t')), \tag{B.6}$$

where  $M_H(z)$  is an even function of the argument,

$$M_H(z) = 1 - \cosh\left(\frac{z}{\tau^*}\right) + \frac{1}{\Gamma(2H + 1)} \left(\frac{|z|}{\tau^*}\right)^{2H} {}_1F_2\left(1; H + 1/2, H + 1; \left(\frac{z}{2\tau^*}\right)^2\right), \tag{B.7}$$

with  ${}_1F_2$  being the generalized hypergeometric function, expressible here in terms of modified Bessel and Struve functions.

Consequently, although the driving noise  $\xi_t^{(MvH)}$  is stationary, the fOUP  $x_t$  itself is nonstationary due to the imposed initial condition  $x_0 = 0$ . If this constraint is relaxed and one considers instead the process defined solely by the first term in equation (B.2) – as is commonly done in the financial mathematics literature (see, e.g. [20]) – one obtains a covariance function that depends only on the time difference  $t - t'$ . In that case,  $x_t$  is a stationary process.

Respectively, the MSD of  $x_t$  obeys, for any  $t$ ,

$$\overline{x_t^2} = \frac{2\Gamma(2H + 1) D' (\tau^*)^{2H}}{\gamma^2} M_H(t). \tag{B.8}$$

The function  $M_H(z)$  exhibits the following asymptotic behavior

$$\begin{aligned} M_H(z) &= \frac{1}{\Gamma(2H+1)} \left( \frac{|z|}{\tau^*} \right)^{2H} + O(z^2), \quad z \rightarrow 0, \\ M_H(z) &= 1 + O\left(e^{-z/\tau^*}\right), \quad z \rightarrow \infty, \end{aligned} \quad (\text{B.9})$$

such that the MSD obeys

$$\begin{aligned} \overline{x_t^2} &= 2D' t^{2H} + O(t^2), \quad t \rightarrow 0, \\ \overline{x_t^2} &= \frac{2\Gamma(2H+1)D'}{\gamma^2} (\tau^*)^{2H} + O\left(e^{-t/\tau^*}\right), \quad t \rightarrow +\infty. \end{aligned} \quad (\text{B.10})$$

## ORCID iDs

Bing Miao  0000-0002-7564-4375

Gleb Oshanin  0000-0001-8467-3226

Luca Peliti  0000-0002-1371-100X

## References

- [1] Uhlenbeck G E and Ornstein L S 1930 On the theory of Brownian motion *Phys. Rev.* **36** 823
- [2] Doob J L 1942 The Brownian movement and stochastic equations *Ann. Math.* **43** 351
- [3] Wang M C and Uhlenbeck G E 1945 On the theory of the Brownian motion II *Rev. Mod. Phys.* **17** 323
- [4] Nørregaard K, Metzler R, Ritter C M, Berg-Sørensen K and Oddershede L 2017 Manipulation and motion of organelles and single molecules in living cells *Chem. Phys.* **117** 4342–75
- [5] Tolić-Nørrelykke S F, Rasmussen M B, Pavone F S, Berg-Sørensen K and Oddershede L B 2006 Stepwise bending of DNA by a single TATA-box binding protein *Biophys. J.* **90** 3694
- [6] Peliti L 2024 *Statistical Mechanics in a Nutshell* 2nd edn (Princeton University Press)
- [7] Peliti L and Pigolotti S 2021 *Stochastic Thermodynamics: An Introduction* (Princeton University Press)
- [8] Mejía-Monasterio C and Rondoni L 2025 *Non-Equilibrium Statistical Mechanics I: Foundations and Modern Applications* (Springer)
- [9] Mardoukhi Y, Chechkin A and Metzler R 2020 Spurious ergodicity breaking in normal and fractional Ornstein-Uhlenbeck process *New J. Phys.* **22** 073012
- [10] Bassanoni A, Vezzani A, Barkai E and Burioni R 2025 Rare events and single big jump effects in Ornstein-Uhlenbeck processes *J. Stat. Mech.* **043201**
- [11] Metzler R, Jeon J-H, Cherstvy A G and Barkai E 2014 Anomalous diffusion models and their properties: non-stationarity, non-ergodicity and ageing *Phys. Chem. Chem. Phys.* **16** 24128
- [12] Metzler R, Grebenkov D and Oshanin G 2024 *Target Search Problems* ed (Springer)
- [13] Mandelbrot B and van Ness J W 1968 Fractional Brownian motions *Fract. Noises Appl. SIAM Rev.* **10** 422
- [14] Biagini F, Hu Y, Øksendal B and Zhang T 2008 *Stochastic Calculus for Fractional Brownian Motion and Applications* (Springer)
- [15] Cheridito P, Kawaguchi H and Maejima M 2003 Fractional Ornstein-Uhlenbeck processes *Electr. J. Probab.* **8** 1–14
- [16] Kaarakka T and Salminen P 2011 On fractional Ornstein-Uhlenbeck processes *Commun. Stoch. Anal.* **5** 121
- [17] Jeon J-H and Metzler R 2012 Inequivalence of time and ensemble averages in ergodic systems: exponential versus power-law relaxation in confinement *Phys. Rev. E* **85** 021147
- [18] Chevillard L 2017 Regularized fractional Ornstein-Uhlenbeck processes and their relevance to the modeling of fluid turbulence *Phys. Rev. E* **96** 033111
- [19] Valov A and Meerson B 2025 Dynamical large deviations of the fractional Ornstein-Uhlenbeck process *J. Phys. A: Math. Theor.* **58** 095002
- [20] Garnier J and Sølna K 2017 Correction to Black-Scholes formula due to fractional stochastic volatility *SIAM J. Financ. Math.* **8** 560
- [21] Feynman R P and Hibbs A R 1965 *Quantum Mechanics and Path Integrals* (McGraw-Hill)
- [22] Wiegell F W 1986 *Introduction to Path-Integral Methods in Physics and Polymer Science* (World Scientific)
- [23] Kleinert H 2004 *Path Integrals in Quantum Mechanics, Statistics, Polymer Physics and Financial Markets* (World Scientific)
- [24] Wio H S 2013 *Path Integrals for Stochastic Processes: An Introduction* (World Scientific)
- [25] de Pirey Th A, Cugliandolo L F, Lecomte V and van Wijland F 2022 Path integrals and stochastic calculus *Adv. Phys.* **71** 1
- [26] Dean D S, Miao B and Podgornik R 2019 Path integrals for higher derivative actions *J. Phys. A* **52** 505003
- [27] Burkhardt T W 2014 First passage of a randomly accelerated particle *First-Passage Phenomena and Their Applications* ed R Metzler G Oshanin and S Redner (World Scientific, Singapore) pp 21–44
- [28] Burlatskii S F and Oshanin G 1988 Probability distribution for trajectories of a polymer chain segment *Theor. Math. Phys.* **75** 659
- [29] Sebastian K L 1995 Path integral representation for fractional Brownian motion *J. Phys. A: Math. Gen.* **28** 4305
- [30] Jumarie G 2007 Path integral for the probability of the trajectories generated by fractional dynamics subject to Gaussian white noise *Appl. Math. Lett.* **20** 846
- [31] Calvo I and Sanchez R 2008 Path integral formulation of fractional Brownian motion for general Hurst exponent *J. Phys. A: Math. Theor.* **41** 282002
- [32] Bénichou O and Oshanin G 2024 A unifying representation of path integrals for fractional Brownian motions *J. Phys. A: Math. Theor.* **57** 225001
- [33] Meerson B, Bénichou O and Oshanin G 2022 Path integrals for fractional Brownian motion and fractional Gaussian noise *Phys. Rev. E* **106** L062102
- [34] Meerson B and Sasorov P V 2024 Fractional Brownian motion in confining potentials: non-equilibrium distribution tails and optimal fluctuations *J. Phys. A: Math. Theor.* **57** 445002

- [35] Meerson B and Sasorov P V 2025 Fractional Brownian motion with negative hurst exponent (arXiv:[2507.05977](https://arxiv.org/abs/2507.05977))
- [36] Lévy P 1953 *Random Functions: General Theory With Special Reference to Laplacian Random Functions* vol 1 (University of California Publications in Statistics) p 331
- [37] Samko S G, Kilbas A A and Marichev A I 1993 *Fractional Integrals and Derivatives: Theory and Applications* (Taylor & Francis Books)
- [38] Meerson B and Oshanin G 2022 Geometrical optics of large deviations of fractional Brownian motion *Phys. Rev. E* **105** 064137
- [39] Lim S C and Sithi V M 1995 Asymptotic properties of the fractional Brownian motion of Riemann-Liouville type *Phys. Lett. A* **206** 311
- [40] Pipiras V and Taqqu M 2000 Integration questions related to fractional Brownian motion *Prob. Theory Relat. Fields* **118** 121
- [41] Zinn-Justin J 2002 *Quantum Field Theory and Critical Phenomena International Series of Monographs on Physics* 4th edn (Clarendon)
- [42] Yaglom A M 1987 *Correlation Theory of Stationary and Related Random Functions* vol 1 (Springer)